Structural Characterization of PLA−PEO−PLA Solutions and Hydrogels: Crystalline vs Amorphous PLA Domains

Sarvesh K. Agrawal,[†] Naomi Sanabria-DeLong,[‡] Gregory N. Tew,[‡] and Surita R. Bhatia*,[†]

Department of Chemical Engineering, University of Massachusetts, Amherst, 686 North Pleasant Street, Amherst, Massachusetts 01003, and Department of Polymer Science and Engineering, University of Massachusetts, Amherst, 120 Governors Drive, Amherst, Massachusetts 01003

Received March 15, 2007; Revised Manuscript Received November 29, 2007

ABSTRACT: We have shown that we can significantly modify the nanoscale structure of solution and gels of ABA triblock copolymers in a solvent selective for the mid B block by making simple changes to the stereochemistry of the A block. We have also shown that the length of the A block can be used as an additional variable to further modify and thereby control the sizes of the nanoscale domains formed by these polymers in the presence of the solvent. Our systems are poly(lactide)−poly(ethylene oxide)−poly(lactide) solutions and gels, which have been previously shown to have tunable release characteristics and mechanical properties suitable for applications in tissue engineering and drug delivery. We have performed SANS to understand the self-assembly of these polymers in aqueous solution as a function of block length and stereospecificity of the PLA block as well as polymer concentration. A significant difference in structure and association behavior was seen between polymers made from amorphous D/L-lactic acid as compared to those with crystalline L-lactic acid blocks. In the former case, spherical micelles with radii of 10−14 nm form, whereas the latter forms assemblies of nonspherical "lamellar micelles" with characteristic radii of 11−15 nm and thicknesses of 8−10 nm. In both cases, increasing PLA block length leads to a larger characteristic size. Both polymers form an associative network structure at higher concentrations, leading to gelation.

1. Introduction

Copolymers of poly(lactide) (PLA) and poly(ethylene oxide) (PEO) have been extensively studied as potential biomaterials because of their nontoxicity, biocompatibility and biodegradability.[1−12] Another property that makes these triblocks suitable candidates for biomedical applications is their ability to form hydrogels when suitable lengths of PLA and PEO blocks are copolymerized. These hydrogel matrices can be injected or implanted in the body and can be made to match the surrounding tissues in mechanical properties, water content, and interfacial tension by adjusting the exact chemistry of the polymers.

ABA block copolymers with small hydrophobic end blocks have been investigated for several years as systems forming associative networks of flowerlike micelles,[9,13−27] which at high concentrations result in formation of elastic gels. Experimental investigations have shown that the microstructure and association behavior of these systems can be controlled by varying the component block lengths, which has a direct effect on the gel properties.

In our group, we recently investigated rheological properties of hydrogels of poly(L-lactide)−poly(ethylene oxide)−poly(L-lactide)[PLA−PEO−PLA].[24−26] We have shown that these polymers formed very strong physically associated gels that are analogous to reversible network gels formed from telechelic hydrophobically modified polymers. However, the hydrophobic PLA domains in these gels are crystalline, leading to more permanent junctions in the network. The elastic modulus of the hydrogels formed was comparable to several native soft tissues and could be easily modified by controlling the PLA block length, thus making these materials very suitable for tissue engineering applications. We have also shown that the rheological properties and drug release behavior of the triblock copolymer gels can be modified significantly by using triblocks synthesized with a racemic mixture of D- and L-lactide instead of optically pure L-lactide blocks.[28,29] Using wide-angle X-ray diffraction (WAXD), we have confirmed that gels formed with a racemic mixture of D- and L-lactide have amorphous PLA domains, while gels formed from L-lactide polymers have crystalline PLA domains.[30] In order to fully understand and control the macroscopic properties of these polymer gels, a detailed understanding of the self-assembled structure of the polymer in solution is required. It is important to determine how the changes in the stereochemistry of the hydrophobic PLA block affect the nanoscale structure of these triblock copolymers in solution in order to understand its effect on the macroscopic properties of solutions and gels formed using these polymers. This relationship between the chemistry of the polymer, its nanoscale structure in solution and its macroscopic properties can thus be utilized to form tailor-made materials useful for specific applications.

Despite widespread interest in these polymers, no detailed studies have been performed to characterize the structure of di- or tri-blocks of PLA and PEO in the hydrogel state. Riley et al. have used small-angle neutron scattering (SANS) experiments to characterize the core−shell structure of PLA−PEG nanoparticles.[9] Some researchers have postulated a plausible gelation mechanism for the same or similar systems based upon the theory of associated network formation,[3,7,9,31] but they have performed no detailed and quantitative characterization of the hydrogel structure.

The self-assembly of block copolymers with a coil−crystalline structure dispersed in solution, where one of the blocks

* To whom correspondence should be sent. E-mail: sbhatia@ecs.umass.edu.

[†] Department of Chemical Engineering, University of Massachusetts, Amherst.

[‡] Department of Polymer Science and Engineering, University of Massachusetts, Amherst.

10.1021/ma070634r CCC: $40.75
Published on Web 02/07/2008

forms crystalline domains, has in particular been of considerable interest;[32−34] however, most of these studies characterize the micellar morphology by casting the polymer on a substrate and observing it by electron microscopy. Even though the micrographs demonstrate the platelet or needlelike structure that is formed by the polymers at different ratios of coil and crystalline blocks, it is understood that the micelles will collapse in the absence of the solvent upon being cast thus affecting the dimensions and morphology of the micelles. Some groups have also investigated the platelet structures of the micelles in solution formed by coil−crystalline diblock copolymers using small angle scattering techniques.[7,35,36] However no detailed investigation has been done on crystalline−amorphous−crystalline triblock copolymers in the presence of a solvent selective for the amorphous midblock and no study is present on the gelation behavior of these materials with increasing concentration of the polymer, which increases cross-linking. Moreover, to the best of our knowledge, no studies have been performed on the differences in structures of associative network hydrogels of ABA triblocks formed using crystalline vs amorphous hydrophobic domains.

Here we report the use of crystallinity of the hydrophobic PLA block to significantly modify the nanoscale structure of PLA−PEO−PLA triblock copolymers in dilute solution and concentrated gel state. The change in structure and association parameters of the gel with changes in stereospecificity and length of hydrophobic PLA block was studied using SANS. The solution and hydrogel structure of polymers with crystalline L-lactide end blocks is seen to be significantly different from those made with amorphous D- and L-lactide end blocks, which accounts for the large difference in their mechanical properties that we have reported previously.[28] Moreover, the length of the PLA block can be varied systematically, which provides an additional handle for influencing the structure and properties of these polymer hydrogels.

2. Materials and Methods

2.1. Materials. Either L-lactide ((3*S*)-*cis*-3,6-dimethyl-1,4-dioxane-2,5-dione) or a racemic mixture of L- and D-lactide (3,6-dimethyl-1,4-dioxane-2,5-dione) from Aldrich was purified by recrystallization in ethyl acetate and then sublimated prior to polymerization. The α,ω-dihydroxy poly(ethylene glycol) macroinitiator with molecular weight 8000 (PEG 8K, Aldrich) was dried at room temperature under vacuum for 2 days prior to polymerization. MALDI and GPC showed this polymer to be 8900 in weight. Stannous octanoate (Alfa Aesar) was used without further purification.

2.2. Synthesis of PLA—PEO—PLA Triblock Copolymer. PLA−PEO−PLA triblock copolymers were synthesized in the bulk. PEO was weighed into a dry round-bottom flask, purged with nitrogen, and placed into an oil bath at 150 °C. Stannous octanoate was introduced to the molten PEO, followed by the immediate addition of lactide to the macroinitiator/catalyst melt. The flask was capped and allowed to polymerize for 24 h at 150 °C while stirring and is then stopped by quenching in methanol. The product was dissolved in tetrahydrofuran and precipitated in hexanes 4 times. The copolymer was then dried under vacuum for 2 days.

The PDI and polydispersity measurements for the polymers synthesized were done as follows. ^{1}H NMR spectra were recorded with a 300 MHz Bruker Spectrospin 300. Chemical shifts were expressed in parts per million using deuterated chloroform solvent protons as the standard. The average degrees of polymerization (DP) were calculated by comparing the integration of the methyne peak of PLA to the integration of the methylene peak of the PEO block. Gel permeation chromatography (GPC) was performed with a Polymer Laboratories PL-GPC50 with 2 PLGel 5 μm Mixed-D columns, a 5 μm guard column, and a Knauer RI detector vs poly(styrene) standards. The eluent was *N*,*N*-dimethylformamide with 0.01 M LiCl at 50 °C.

Table 1. Characteristics of PLA−PEO−PLA Triblock Copolymers Synthesized

sample name	DP_{PLA}	DP_{PEO}	MW	crystallinity of PLA block
58L	58 (PLLA)	202	13.0K	crystalline
72L	72 (PLLA)	202	14.1K	crystalline
77L	77 (PLLA)	202	14.4K	crystalline
88L	88 (PLLA)	202	15.2K	crystalline
66R	66 (PRLA)	202	13.7K	amorphous
72R	72 (PRLA)	202	14.0K	amorphous
88R	88 (PRLA)	202	15.2K	amorphous
92R	92 (PRLA)	202	15.5K	amorphous

The polymer series that we used in our study are listed in Table 1. We systematically varied two parameters, the MW and crystallinity of the hydrophobic PLA block. We have verified the crystallinity of the PLA domains in the hydrogel state using WAXD and presented these data in a previous publication.[30] The polymers with crystalline L-lactic acid blocks are denoted the L-lactide series polymers, and those made from a racemic mixture of D-/L-lactic acid are denoted as *rac*-lactide series polymers. Within each series the PLA block lengths has been suitably chosen to match the polymer MW in the other series for easy comparison. The sample names indicate the total length of PLA block followed by a letter indicating the stereo specificity of PLA block, e.g., 58R refers to the polymer $PLA_{29}PEO_{202}PLA_{29}$ in the *rac*-lactide series which is amorphous while 58L refers to the polymer $PLA_{29}PEO_{202}PLA_{29}$ in the L-lactide series which has crystalline PLA domains. The polydispersity index (PDI) for all the polymers synthesized was reasonably low and was less than or equal to 1.21 for all samples. The PDI of the PEO block purchased was 1.04.

2.3. Preparation of Polymer Solutions and Gels. In a typical method of sample preparation, the required amount of polymer was added to D_2O and was then stirred for a day at room temperature. The sample was then heated at 80 °C for 20 h and subsequently stirred for 1−2 days at room temperature to allow for equilibration. For each polymer studied, samples were made at concentrations of 0.5%, 2%, 10%, 22%, and 30% by weight.

We also prepared select samples with different thermal histories to determine whether sample preparation would play any role in the nanoscale assembly. We did not observe any significant differences in the spectra of samples prepared at different temperatures. We have not included this data due to space considerations. We have previously observed micrometer-sized aggregates in these gels, and formation of these aggregates is likely related to how well the preparation method "breaks up" larger crystallites into individual micelles. We suspect that the large-scale assembly and structure of these systems may be strongly affected by thermal history; however, it appears that the nanoscale assembly is not strongly affected.

2.4. SANS Experiments. Small-angle neutron scattering (SANS) measurements were conducted on the small angle scattering instrument (SASI) at the Intense Pulsed Neutron Source located at Argonne National Laboratory, Argonne, IL[37] and on the 30 m small-angle neutron scattering instrument at the NG-3 beamline at the National Institute for Standards and Technology (NIST), Gaithersburg, MD.[37] Scattering length densities (ρ_b) used for calculations are 1.73×10^{-6}, 6.38×10^{-7}, and 6.36×10^{-6} Å^{-2} for PLA, PEO, and D_2O respectively. The scattering length density of the monomers are calculated as $\rho_b = (\rho b N_{AV})/M$, with N_{AV} being Avogadro's number, b the total scattering length of all the atoms in the monomer, ρ the bulk density of the polymer, and M the monomer molecular weight. Spectra were obtained at 25 °C for all the samples. Quartz sample cells with a path length of 1 and 2 mm were used for the concentrated and dilute samples, respectively. Spectra were collected for one to 4 h, depending on the sample concentration and contrast. Deuterated water or a mixture of D_2O/H_2O in a predetermined ratio (for contrast matched samples) was used to quantify the solvent scattering. The q range covered in these

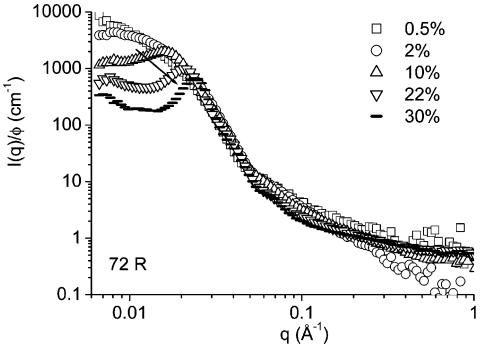

Figure 1. Change in SANS spectra with increasing concentration of 72R polymer in D_2O.

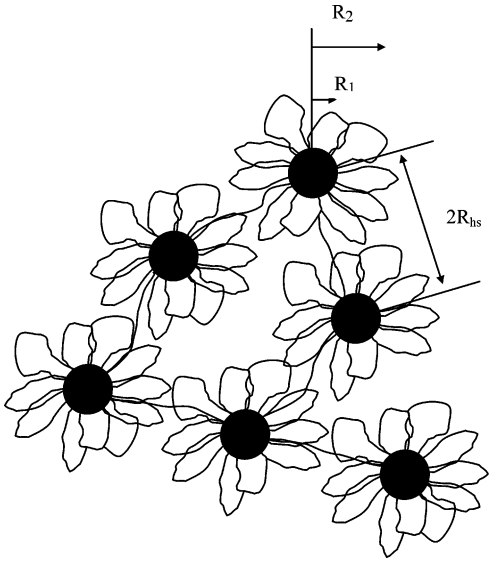

Figure 2. Representation of the network that is formed when neighboring micelles of the *rac*-series triblocks associate. The micelle cores are amorphous PLA domains.

experiments was 0.005 $Å^{-1} < q < 1.0$ $Å^{-1}$. The sample to detector distance was 1.44 m. Additional contrast-matching experiments were performed that involved collecting the scattering data for the same polymers at different contrast conditions while keeping the sample environment same as described above. The q range covered in these experiments was 0.005 $Å^{-1} < q < 0.1$ $Å^{-1}$. Data reduction and normalization were performed using standard techniques,[37] and all SANS data reported herein are on an absolute scale except where noted.

3. Results and Discussions

3.1. Model Independent Analysis of Scattering Data. *rac*-Lactide Series Polymers. SANS experiments were carried out on the *rac*-series polymers at concentrations of 0.5%, 2%, 10%, 22%, and 30% by weight to compare the effect of micelle formation and packing. A representative set of scattering spectra for 72R polymer at all the concentrations is shown in Figure 1 after scaling with the respective volume fraction. At the lowest concentration of 0.5 wt %, no correlation peak is seen in the scattering spectrum. The spectrum is consistent with that of spherical entities in solution. Amphiphilic triblock copolymers with ABA architecture and small end blocks are known to form flowerlike micelles in a solvent selective for the midblock.[13,38] The end blocks, which are incompatible with the solvent, form the core of the micelles whereas the midblock forms the corona. PLA−PEO−PLA triblocks with amorphous PLA domains are expected to form such spherical micellar aggregates at low concentrations in aqueous solutions because PLA is hydrophobic and PEO is hydrophilic. Thus, the scattering from low concentration solutions of the polymer is expected to be obtained from these spherical aggregates. As the concentration of polymer is increased, the micelles come closer to each other and begin to interact, resulting in a correlation peak. We expect that the micelles will associate with neighboring micelles through the hydrophobic end blocks to form a reversible network. This leads to liquid-like ordering of the micelles, which results in a correlation peak for concentrations above 10 wt %. This peak, which is representative of the average distance between scattering centers in the gel, becomes sharper and shifts to higher wave vectors, q, with increasing concentration (Figure 1) thereby indicating a decrease in intermicellar spacing as the micelles become more closely packed and the bridges between them increase in number. Increasing the number of bridges eventually leads to formation of a well-connected network of micelles (Figure 2), thereby leading to formation of a gel at high concentrations. A plot of the scattering spectra for the different *rac*-lactide series polymer gels at 30 wt % concentration is shown in Figure 3. All systems with amorphous PLA domains show similar characteristic scattering spectra. The spectra also overlap over each other for almost the entire q range, indicating that all the polymer gels have similar nanoscale structure and can be analyzed using the same physical model.

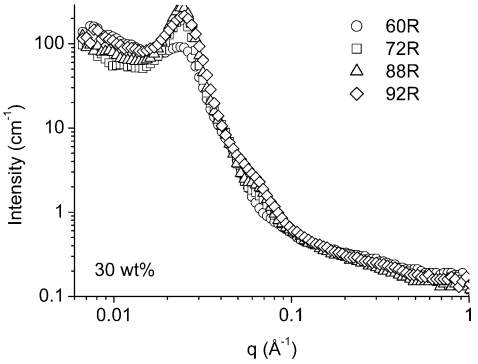

Figure 3. Change in SANS spectra with increasing PLA block length of *rac*-lactide series polymer solutions in D_2O.

3.2. Data Analysis: Model Fits to SANS Data. *rac*-Lactide Series Polymers. The overall scattering intensity of the micelle solution can be written as a product of the form factor ($P(q)$) and the structure factor effects ($S(q)$), in addition to an incoherent background scattering (bkg) term.

$$I(q) = N(\Delta\rho)^2 P(q) S(q) + \text{bkg} \quad (1)$$

Here N is the number density of scattering centers (micelles), and $\Delta\rho$ is the contrast of the scattering length density (SLD) between the micelle particle and the solvent. Structure factor effects, given by $S(q)$, arise from long-range correlations between the scattering centers, and $S(q)$ is unity at low polymer concentrations but may have a significant effect on the scattering profile at high concentrations. At low concentrations, the scattering profile is governed by the form factor, which is a function of the particle shape. Scattering spectra obtained from spherical micelles formed by amphiphilic copolymers has very commonly been described by the core−shell form factor model,[38−41] given by eq 2.[42] This model accounts for a spherical core of radius R_1 surrounded by a spherical shell of radius R_2 with the assumption of homogeneous scattering length densities (SLD) within the core and the shell. The model also accounts for the difference in contrast between the core and shell and between the shell and surrounding medium (D_2O). In our study

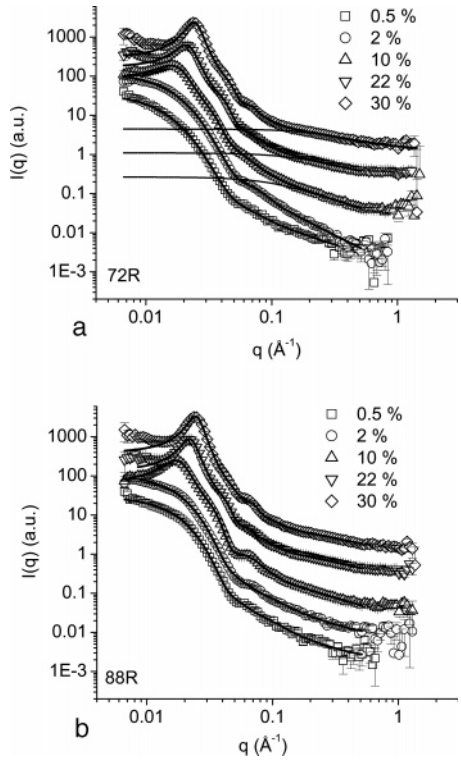

Figure 4. Representative fits of the scattering spectra for 72R (a) and 88R (b) polymers at different concentrations to the core−shell form factor model. At higher concentrations the interactions between micelles are described by the hard sphere structure factor model. The fits are shown by the heavy solid lines, and the lighter lines in (a) indicate the contribution of eq 5 to the fit function.

the core is formed by amorphous PLA, the shell is formed by PEO, and D_2O forms the surrounding medium.

$$(\Delta\rho)^2 P(q) = \left[\frac{4}{3}\pi {R_1}^3(\rho_1 - \rho_2)\frac{3j_1(qR_1)}{qR_1} + \frac{4}{3}\pi {R_2}^3(\rho_2 - \rho_s)\frac{3j_1(qR_2)}{qR_2}\right]^2$$

$$j_1(x) = \frac{\sin(x) - \cos(x)}{x^2} \tag{2}$$

Here ρ_1, ρ_2, and ρ_S are the scattering length densities of the core, corona and solvent, respectively. Polydispersity (σ) in the size of micelles is introduced in this model by averaging the form factor over a Shultz distribution of radii. The SLDs of the core and shell regions in the above model are determined by the polymer compositions in the two regions and their degree of hydration.[39,43,44] However, simultaneous determination of the core and shell radius and their degree of hydration gives ambiguous results.[39] We overcome this problem by assuming that the core is only formed by well-packed PLA chains and is not hydrated, thereby reducing the model parameters to just three, the core and shell radius and polydispersity in micelle size. This is a reasonable assumption since PLA is very hydrophobic and is also consistent with the results obtained by Riley et. al which show that PLA−PEO diblocks form micelles with anhydrous PLA cores.[9] The aggregation number (N_{agg}), or the number of polymer chains forming the core, can then straightforwardly be obtained by using the values of the core radius and the density of dry PLA, with the use of the relation

$$N_{agg} = \frac{4/3\pi {R_1}^3}{V_{PLA}} \tag{3}$$

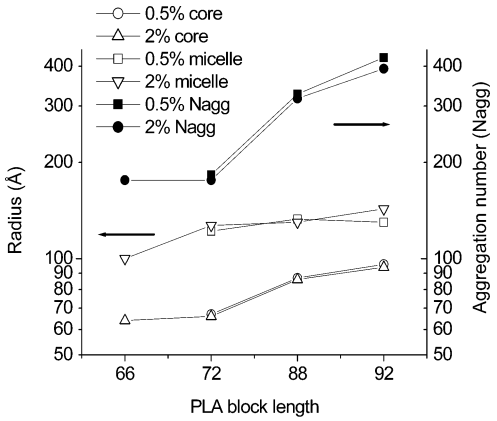

Figure 5. Change in micellar dimensions and aggregation number with increasing PLA block length.

The degree of hydration of the shell (ϕ_{sh}) can now be calculated with use of this value of N_{agg}, the shell radius and density of dry PEO[39,40]

$$\phi_{sh} = 1 - \frac{N_{agg}V_{PEO}}{{}^4/_3\pi({R_2}^3 - {R_1}^3)} \tag{4}$$

Here V_{PLA} and V_{PEO} are the molecular volumes of PLA and PEO respectively. The assumption of an anhydrous PLA core was taken into account by fixing the SLD of the core to the known SLD value of amorphous PLA. The SLD value of the surrounding matrix that includes water and PEO was then allowed to float during the data fitting process. The parameters of the fitting program were adjusted to obtain best fits of the model to the data using a least-square fitting approach.

We used the above model to fit our data for *rac*-lactide series polymers at dilute concentration (0.5 and 2 wt %) at which the structure factor $S(q)$ can be assumed to be 1 and only form factor effects dominate. The fits were seen to be good in the low and mid q regime, but deviate slightly at the high q. This is due to the assumption of homogeneous scattering length densities for the core and the shell, which does not take into account the internal polymer structure and monomer−monomer interactions of the chains in solution. Because of this, the model breaks down at values of q higher than the inverse correlation length of the internal structure of polymers chains in a solvent.[45,46] Pedersen and Gerstenberg have proposed a model for polymer coated homogeneous spheres as a representation of block copolymer micelles[47] which has four terms in the form factor; one from the homogeneous spheres, one from polymer chains and two cross terms corresponding to chain−chain and chain-sphere interactions. The contributions from the cross terms is generally small and can be omitted. Thus, the term corresponding to internal polymer structure can be taken into account in the core−shell model by adding the contribution due to monomer−monomer correlations or blob scattering ($(I(q)_{exc}$), which is given as[36,48]

$$I(q)_{exc} = \alpha(\rho_2 - \rho_s)^2 \frac{\sin(\mu\tan^{-1}(q\xi))}{q\xi(1 + (q\xi)^2)^{\mu/2}} \tag{5}$$

Here ξ is the average correlation length of polymer internal structure (blob size), $\mu = 1/\nu - 1$ ($\nu = {}^3/_5$ for polymer chains in a good solvent) and α is a scaling prefactor. Effectively at large q values, eq 5 varies as $q^{-1/\nu}$.

Excellent fits to the data were obtained with the use of the modified form factor model. Representative fits for the 72R

Table 2. Micelle Parameters Obtained by Fitting the Scattering Spectra for *rac*-Lactide Series Polymers at Different Concentrations to a Physical Model

	66R					72R				
param										
concn (wt %)	0.5	2	10	22	30	0.5	2	10	22	30
R_1 (Å)		64.2 ± 0.7	61.9 ± 0.1	61.8 ± 0.2	58.7 ± 0.3	67 ± 5.9	66.2 ± 1.2	80.6 ± 0.5	67.2 ± 0.6	77.1 ± 0.3
R_2 (Å)		100 ± 1.8	110.3 ± 0.4	101.9 ± 1	105.3 ± 0.6	121.9 ± 8.7	127.2 ± 1.9	137.2 ± 1.2	119.5 ± 0.8	130 ± 1.1
$R_2 - R_1$ (Å)		35.9 ± 1.7	48.4 ± 0.4	40.1 ± 0.9	46.6 ± 0.6	54.8 ± 6.4	61 ± 1.5	56.6 ± 1.1	52.3 ± 0.6	52.9 ± 1.1
σ		0.31	0.23	0.21	0.23	0.36	0.27	0.28	0.3	0.22
N_{agg}		176	157	156	135	183	176	318	184	279
ϕ_{sh}		0.26	0.56	0.41	0.57	0.62	0.69	0.52	0.59	0.5
R_{hs} (Å)			134	114	105			167	143	130
ξ (Å)		15.7 ± 3.7	8.4 ± 0.3	5.6 ± 0.4	3.1 ± 0.2	11.2 ± 2.8	16.7 ± 2.5	8.5 ± 0.3	5.4 ± 0.2	3.3 ± 0.2

	88R					92R				
param										
concn (wt %)	0.5	2	10	22	30	0.5	2	10	22	30
R_1 (Å)	87 ± 1.6	86.1 ± 0.8	83.7 ± 0.2	79.8 ± 0.3	84.6 ± 0.2	96.3 ± 4.4	93.8 ± 0.3	80.8 ± 0.4	80 ± 0.4	86.8 ± 0.2
R_2 (Å)	133.4 ± 3.6	130.4 ± 2.1	145.9 ± 0.4	131.3 ± 0.7	133.1 ± 0.8	130.5 ± 14.5	143.7 ± 1.7	107.7 ± 90.8	111 ± 25.9	134.5 ± 6.8
$R_2 - R_1$ (Å)	46.6 ± 3.3	44.4 ± 1.9	62.3 ± 0.3	51.5 ± 0.6	48.5 ± 0.8	34.1 ± 13.8	49.9 ± 1.7	26.9 ± 90.8	31 ± 25.9	47.7 ± 6.9
σ	0.23	0.24	0.19	0.24	0.18	0.24	0.23	0.31	0.36	0.19
N_{agg}	327	317	292	253	301	426	393	251	243	312
ϕ_{sh}	0.4	0.37	0.64	0.55	0.46	0	0.43	0	0.11	0.45
R_{hs} (Å)			167	142	130			139 ± 1	108	120
ξ (Å)	22.2 ± 17.7	18.4 ± 5.9	6.2 ± 0.2	4 ± 0.2	4.2 ± 0.2	15.1 ± 18	12.3 ± 1.3	5.3 ± 0.6	3.5 ± 0.3	4 ± 0.3

system are shown in Figure 4 and the fit parameters obtained are summarized in Table 2. Figure 4a also shows the contribution of eq 5 to the overall fit function. The equation represents the scattering data very well in the high q regime and has negligible effect on the fit function values in the mid and low q ranges where the contribution due to the core−shell model dominates, using which accurate model parameters related to micelle size can be obtained.

The pronounced correlation peak evident in all the *rac*-lactide series polymer solutions at and above concentrations of 10 wt % is indicative of interactions between micelles and liquid-like ordering in the system and we thus need to take the structure factor, $S(q)$, into account. We describe the interaction effect to the scattering spectra with the use of a hard sphere interaction potential, which has frequently been used for polymeric micellar systems.[39,40,44,46] The Percus−Yevick approximation[49] provides an analytical expression for $S(q)$ with the use of this potential, given as

$$S(q) = \frac{1}{1 + 24G(x,\phi)/x} \tag{6}$$

G is a function of $x = 2qR_{hs}$ and micelle volume fraction ϕ and is given as

$$\begin{aligned} G(x,\phi) = {} & (\alpha(\phi)/x^2)[\sin x - x\cos x] + \\ & (\beta(\phi)/x^3)[2x\sin x + (2 - x^2)\cos x - 2] + \\ & (\gamma(\phi)/x^5)[-x^4\cos x + 4[(3x^2 - 6)\cos x + \\ & (x^3 - 6x)\sin x + 6]] \end{aligned} \tag{7}$$

where α, β, and γ are

$$\alpha = (1 + 2\phi)^2/(1 - \phi)^4$$

$$\beta = -6\phi(1 + \phi/2)^2/(1 - \phi)^4$$

$$\gamma = (\phi/2)(1 + 2\phi)^2/(1 - \phi)^4$$

In principle, the above equation is applicable for monodisperse hard spheres, but it has been used as a very good closed form approximation for polydispersed systems as well.[50]

In order to reduce the fitting parameters, other researchers have set the hard sphere interaction radius (R_{hs}) equal to the total micelle radius (R_2). However for our system, the average intermicellar spacing was seen to vary with concentration, and thus R_{hs} was kept as an independent parameter different from R_2. The fits of the model to the data thus obtained are shown in Figure 4, parts a and b, and the model parameters are given in Table 2.

Discussion of the Results for *rac*-Lactide Series. The total size of the micelles ($2R_2$) obtained from the fits was seen to range from approximately 20 nm for 66R to 29 nm for 92R. The increase in micelle size is primarily due to an increase in size of the PLA core accompanied by an increase in the aggregation number of the micelle, whereas the size of the PEO shell ($R_2 - R_1$) remains in the narrow range of 4.5−6 nm for all samples (Figure 5). It is notable that the micelle size parameters do not change significantly even though they are obtained independently for data sets at different concentrations. Polydispersity in micelle sizes is seen to range between 20 and 30%. The values of aggregation number obtained are large and are in the same range as those reported by Riley et al.[9] The large aggregation numbers also represent that the PLA domains are strongly phase-separated into the micellar core, which is also why these numbers increase as the molecular weight of the hydrophobic block increases and suggests why bridging would be expected to occur in this system. Furthermore, the increase in aggregation number with PLA block length (Figure 5) also shows that the system has a stronger tendency to aggregate at larger PLA block lengths. This is consistent with our observation of an increase in characteristic relaxation times of the *rac*-lactide series hydrogels with increasing PLA block lengths, indicating that stronger junctions are formed in the gels with longer PLA blocks.[28] The increase in micelle aggregation number with increasing PLA block length also agrees with what has been observed in other amphiphilic triblock systems.[51,52] The corona of the micelles is seen to be significantly hydrated with the degree of hydration being more than 50% in most of the cases. We observe that the micellar dimensions do not change with increasing polymer concentrations. However, interactions between the micelles are affected, as is seen by intense scattering at low q values leading to formation of a peak

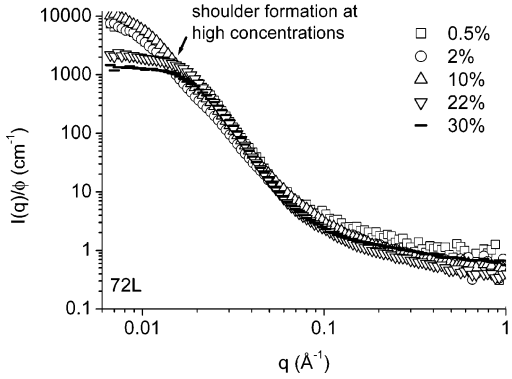

Figure 6. Change in SANS spectra with increase in concentration of 72L polymer in D_2O. The arrow indicates formation of a broad shoulder at high concentrations of the polymer.

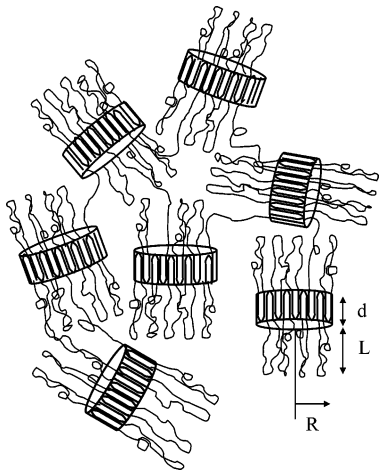

Figure 7. Representation of the network of "lamellar micelles" formed in the case of L-lactide series polymers at high concentrations. The micellar cores can be seen to be randomly orientated.

at concentrations of 10 wt % and shift in this peak position with increasing concentration. This is in consonance with what has traditionally been observed as an indication of attractive interactions or bridging at high concentrations for ABA triblock copolymers in a solvent selective for the midblock.[50,51] In a highly concentrated, well-packed system, the center-to-center distance between any two adjacent micelles interacting via hard sphere repulsions would be expected to be equal to the micelle diameter. This is seen to be precisely true for hydrogels at 30 wt % concentration where the micellar radius (R_2) was seen to be almost identical with the interaction radius (R_{hs}) for all the *rac*-lactide systems. However, at lower concentrations the intermicellar radii were seen to be larger than the micelle radii, indicating that the micelles are not closely packed at those concentrations. The micelles repel each other due to osmotic forces, which are balanced by the attractive forces of the bridges joining them.[13,53] At low concentrations, only a small number of chains are elastically active and form bridges, leading to a broad scattering peak because of polydispersity in the intermicellar distances. As more bridges form in the system at high concentrations, the intermicellar distances become less polydisperse and are governed by the polymer chain length. This results in a sharp scattering peak. These results are also consistent with the rheological characterization of these systems, which show that these polymers form strong associative network hydrogels at high concentrations.[28,30] The values obtained for blob size or "monomer−monomer" correlation distance (ξ) for locally concentrated polymer chains having excluded volume interactions between them are seen to range from 11 to 22 Å for the different systems at low concentration, which is similar to values that have been described by other researchers.[36,46] However, the values of ξ estimated at higher concentrations are found to be very small. These small values of ξ obtained with increasing concentrations can be explained in terms of scaling relations for "concentration blob" as described by Doi,[54] according to which the spatial distances over which a polymer coil displays good solvent scaling becomes smaller with increasing concentrations and the values of ξ scales as, $\xi \sim (c/c^*)^{-3/4}$ with respect to concentration (c). Here c^* is the overlap concentration. Nevertheless, we do not discount the possibility of large errors in the values of ξ obtained due to the interplay between different scattering contributions and errors introduced due to background scattering in the high q regime.

L-Lactide Series Polymers. A significant difference in the nanoscale structure of hydrogels formed by *rac*- vs L-lactide polymers was seen as depicted by the difference in scattering spectra of the L-lactide (Figure 6) and *rac*-lactide series polymers gels. This is consistent with the difference in rheological properties of the two series of hydrogels that we have observed earlier.[30] Specifically, no correlation peak was seen to form in these systems as the concentration of polymer was increased, though formation of a shoulder was clearly evidenced in the low q regime indicated by an arrow in Figure 6. In the mid q region the scattering spectra overlap, which shows that the internal structure or the form factor of the aggregates in solution does not change as the concentration is increased. The shoulder can be viewed as a very broad correlation peak, which forms as structure factor effects set in. The formation of the shoulder represents a broad polydispersity in the interaggregate spacing in the case of L-lactide series polymers. This polydispersity in correlation length is attributed to crystallinity of the L-lactide block in solution. Our WAXD studies have confirmed that PLLA domains in solution and hydrogel state are crystalline[30] and the high elasticity of the L-lactide series hydrogels was attributed to the strong crystalline junctions formed by these materials similar to PVA hydrogels.[55] Thus, in this case, the tendency of PLA blocks to crystallize is another factor leading to aggregation in the system, in addition to the incompatibility of PLA domains with water, which is the cause for aggregation in the *rac*-lactide series gels. The PEO chains are expected to align as brushes on the back of crystalline PLLA lamellae as has been observed for other semicrystalline polymers,[35,36] forming randomly oriented "lamellar micelles" (Figure 7). These chains associate with neighboring lamella to form a network structure at high concentrations similar to that formed in *rac*-lactide series polymers. Formation of such "lamellar micelles" has been described earlier by other groups for systems of diblock copolymers that form aggregates with one of the blocks as crystalline.[7,32−36] Because of random orientation of the lamellae and possible polydispersity in their sizes, no well-defined correlation length exists in these systems and hence no peak is observed in their SANS spectra (Figure 7). This picture is also very strongly supported by data from contrast-matching experiments, described at the end of this section. The contrast matching experiments clearly demonstrate that the micelle cores formed by crystalline PLA segments have a two-dimensional nature, with scattering spectra that have a slope of −2.4 in the mid and high q range.

The SANS spectra of various polymers in the L-lactide series overlap in the mid q range (Figure 8), showing that the form factor of the cross-linked aggregates formed remains unchanged on increasing the length of the PLLA block.

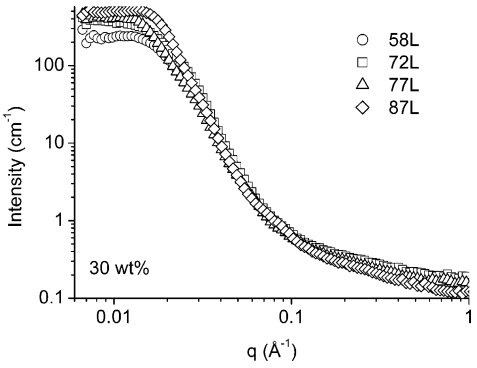

Figure 8. Change in SANS spectra with increase PLA block length of L-lactide series polymer solutions in D_2O.

Data Analysis: Model Fits to SANS Data. The data for L-lactide series polymers was found to be very difficult to fit because there are no strong structural features present in the scattering spectra of this system. It was not possible to fit the data with models for spherically symmetric systems. Moreover, data from contrast matching experiments, described below, clearly confirms that the micelle cores are two-dimensional objects. "Lamellar micelles" as described above resemble a system of thin disks having polymer layers adsorbed or grafted on each surface of the disk. Thus, overall a core−shell model of thin disks, where the core approximates the crystalline PLA polymer segment and the shell represents the layer of PEO chains, can represent the form factor of the system. This scattering function based on the form factor for disklike structures[56] can be represented as

$$I(q) = N \int_0^{\pi/2} [\Delta\rho_s(V_s f_s(q) - V_c f_c(q)) + \Delta\rho_c V_c f_c(q)]^2 S(q) \sin\phi \, d\phi + \text{bkg} \quad (8)$$

$$\langle f_s^2(q)\rangle_\phi = \int_0^{\pi/2} \left[\left(\frac{\sin(q(d/2+L)\cos\phi)}{q(d/2+L)\cos\phi}\right) \times \left(\frac{2J_1(qR\sin\phi)}{qR\sin\phi}\right)\right]^2 \sin\phi \, d\phi \quad (9)$$

$$\langle f_s^2(q)\rangle_\phi = \int_0^{\pi/2} \left[\left(\frac{\sin\left(\frac{qd}{2}\cos\phi\right)}{\frac{qd}{2}\cos\phi}\right)\left(\frac{2J_1(qR\sin\phi)}{qR\sin\phi}\right)\right]^2 \sin\phi \, d\phi \quad (10)$$

In the above equation subscripts s and c represent shell and core respectively. Here d, L, and R are the thickness of the crystalline core, thickness of the shell, and radius of the assumed disk-like core respectively. Since the individual disks or "lamellar micelles" can be randomly oriented in the solution or gel state, the form factors have been orientationally averaged by integrating over ϕ, where ϕ is the angle between the normal to the face of the disks and scattering vector q. A similar function has been used by Richter et al. to represent scattering data from aggregates of poly(ethylene)-poly(ethylenepropylene)(PE-PEP) in selective solvent with crystalline PE cores[36] and by Nelson et al. for systems of adsorbed PEO layers on disklike laponite nanoparticles.[57]

As described earlier, an increase in concentration of the polymer leads to formation of a networked gel because of association between the different PLA crystalline cores. Such

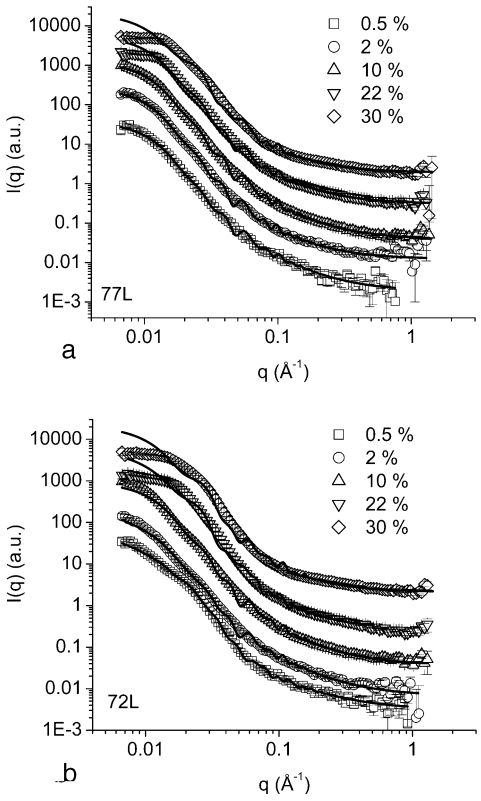

Figure 9. Representative fits of the scattering spectra for 77L (a) and 72L (b) polymer at different concentration to the core−shell form factor model for thin disks convoluted with a structure factor term described for a stack of discs.

"macro-aggregation" leads to convolution of the structure factor effects with the form factor in the small angle scattering spectra of the gels and can be seen in the reduction of the scattering intensity in the low q regime with increasing concentration. For a perfect infinite stack of crystalline disks a maximum in the intensity is expected to be seen at $q_{max} = 2\pi/D$ where D is the period of stacking. However, for finite stacks, it is likely that the disks are randomly oriented and have a variation in the inter-platelet distance in the hydrogel. Thus, to account for both the random variations in a stack of core−shell disks filling up the space in the gel, a structure factor proposed by Kratky and Porod[58] is used, which is given as

$$S(q) = 1 + \frac{2}{n}\sum_{k=1}^{n}(n-k)\cos(kDq\cos\phi) \times \exp[-k(q\cos\phi)^2\sigma_D^2/2] \quad (11)$$

Here n is the number of disks in the stack, D is the period of stack and σ_d is the term for Gaussian smearing of the stacking period due to distance variations between disks. Averaging of the intensity function is done over ϕ to account for random orientation of the platelets. In order to reduce the total number of fitting parameters, D is set equal to $d+2L$. Finally, blob scattering seen at high q values is taken into account by adding the term in eq 5 to the total scattering intensity (eq 8).

The aggregation number of the chains forming the lamellar micelle was calculated by using the dry density of crystalline PLA in the following equation;

$$N_{agg} = \frac{V_{cr}}{V_{PLA}} \quad (12)$$

Table 3. Micelle Parameters Obtained by Fitting the Scattering Spectra for L-lactide Series Polymers at Different Concentrations to a Physical Model

	58L					72L				
param										
concn (wt %)	0.5	2	10	22	30	0.5	2	10	22	30
R (Å)	114.1 ± 0.7	113.6 ± 0.3	134.2 ± 0.1	114	114	119.3 ± 0.6	137.4 ± 0.3	135.1 ± 0.1	138	138
d (Å)	85.8 ± 2.4	82.9 ± 1.1	95.9 ± 0.5	85	85	89.3 ± 1.5	95.5 ± 1.3	96.5 ± 0.5	96	96
L (Å)	121.6 ± 1.1	119.2 ± 0.6	137.9 ± 0.3	124.1 ± 0.1	128.3 ± 0.1	131.9 ± 0.8	144.5 ± 0.7	141.9 ± 0.3	157.7 ± 0.1	143 ± 0.1
N_{agg}	653	625	1009	645	645	598	848	830	860	860
ϕ_{sh}	0.14	0.15	0.15	0.17	0.19	0.34	0.35	0.33	0.40	0.34
N	5 ± 1.8	2.2 ± 0.17	1	1	1	11.1 ± 4.07	2	1	1	1
σ_d (Å)	50.8 ± 2.1	48.2 ± 1.6	0	0	0	55.5 ± 1.31	79.5 ± 2.7	0	0	0
ξ (Å)	16.4 ± 2.3	24.8 ± 1.1	38.4 ± 0.3	29.8 ± 0.5	31.6 ± 0.6	10.4 ± 1.5	35.5 ± 0.5	40.5 ± 0.3	30 ± 0.3	40.2 ± 0.5

	77L					87L				
param										
concn (wt %)	0.5	2	10	22	30	0.5	2	10	22	30
R (Å)	143 ± 0.5	149.4 ± 0.2	145.2 ± 0.1	143	143		131.2 ± 0.2	130.8 ± 0.1	131	131
d (Å)	92.3 ± 3.4	99.4 ± 1.2	98.4 ± 0.5	92	92		102.7 ± 0.6	98.4 ± 0.4	102	102
L (Å)	156.5 ± 1.7	162 ± 0.6	159.8 ± 0.3	157.3 ± 0.1	161.4 ± 0.1		150.7 ± 0.4	143.4 ± 0.2	144.9 ± 0.1	147.1 ± 0.1
N_{agg}	832	976	913	828	828		689	657	682	682
ϕ_{sh}	0.46	0.44	0.44	0.47	0.48		0.45	0.44	0.43	0.44
N	1	1	1	1	1		11.6 ± 4.4	3	1	1
σ_d (Å)	0	0	0	0	0		53.9 ± 1.4	74.4 ± 0.8	0	0
ξ (Å)	60.9 ± 2.2	47.6 ± 0.7	42.8 ± 0.3	47.4 ± 0.2	47.3 ± 0.3		6.2 ± 0.8	13.13 ± 0.1	21.7 ± 0.2	26.7 ± 0.2

where $V_{cr} = \pi R^2 d$. Subsequently the volume fraction of water in the shell or the amount of hydration of the PEO chains is calculated using the following equation

$$\phi_{sh} = 1 - \frac{N_{agg} V_{PEO}}{V_L} \tag{13}$$

where $V_L = 2\pi R^2 L$. Least-square fits of the model to the data were obtained by setting the SLD's of the PLA and PEO to their original values, whereas the SLD of the solvent was fit. A representative set of fits of the above model to scattering spectra for 77L and 72L polymer solutions and gels is shown in Figure 9, parts a and b respectively. The fit parameter values obtained are presented in Table 3 and are discussed below.

Discussion of the Results for the L-Lactide Series. A quantitative determination of the micellar parameters was done by fitting the scattering data to the model described above. The model provided a satisfactory fit to the experimental scattering profiles at low concentrations. In particular, the profiles were seen to be very sensitive to the micellar structure parameters including R, d, and L. The values of R, d, and L were obtained independently at different concentrations for each of the polymer samples and in each case the values obtained were in reasonable agreement of each other. The crystallite diameters were found to lie in the range of 22−30 nm and the thickness of the core was seen to be in the range 8−10 nm. The crystallite diameters agree well with the crystallite length of 23.0 nm estimated from XRD data on a gel of 62L polymer that was prepared using the same synthetic technique and thermal history as the samples in this study.[59] This gives us confidence in both the model used to fit the data and the quantitative values of the parameters. In addition, Fujiwara et al. have previously observed morphology of aggregates formed by PLLA−PEO diblock copolymers cast on mica surface through AFM. The size of the aggregates, which were cast from solutions of the polymer at concentrations above 0.1 wt %, were seen to have a discoid shape and dimensions of 30−50 nm in total diameter and 5−10 nm in thickness.[32] Upon annealing at 60 °C for 2 h in a process similar to ours, the aggregates rearrange and these particles were seen to form crystalline band structures with sizes of 5−15 nm. Even though the casting of the aggregates on the mica surface from solution is expected to affect the morphology of these particles, it is still notable that the crystallite dimensions and its expected shape obtained by us through modeling of the small angle scattering data for solutions and gels matches well with the observations described above.

Halperin and co-workers[60] and Lin and Gast[7] provided scaling models for coil−crystalline polymers in solution, which provide us with a theoretical framework to aid in understanding these results. In their models, they considered a core formed by folded crystalline polymer chains. Since the amorphous polymer chains are tethered to the crystalline core at the core−corona interface, the number of folds of the polymer chain determines the amorphous polymer density in the corona region. If the core is thicker with fewer folds, the tethering density of the amorphous chains increases, leading to repulsion between them which causes stretching of the amorphous blocks. Such strong repulsions can be avoided by larger numbers of chain folds in the crystalline core, which in turn would reduce lamellar thickness. However, increase in lamellar size also increases the core−solvent interfacial energy, which is to be minimized. Thus, the thickness of the lamellae in this case is governed by a balance between an entropic contribution due to stretching of solvated chains and an enthalpic contribution due of folding of semicrystalline chains in the lamellae.

For a constant length of the amorphous polymer block, the number of folds of the crystalline block remains constant and the crystallite thickness (d) would increase with increasing molecular weight of crystalline block. The resulting scaling relationship described by Lin and Gast[7] using a mean field approximation is given as $d \sim N_A N_B^{-3/5} E_{fold}^{3/5}$. Here N_A and N_B are the number of monomers in crystalline and amorphous blocks, respectively, and E_{fold} is the energy cost to create a crystalline fold. The crystallite core thickness found by our calculation was also seen to increase linearly with increasing PLA block length, in agreement with the above observation (Figure 10). The aggregation number of the micelles was seen to be much larger than that for *rac*-lactide series polymers of similar molecular weight (Table 2). Larger aggregation numbers are expected for the crystalline polymers because of higher driving force for aggregation as compared to the amorphous polymers (Figure 11). The size of the PEO layer was found to

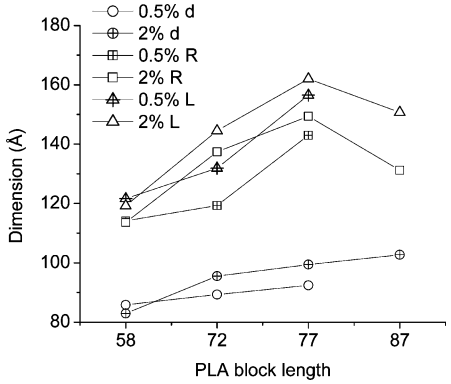

Figure 10. Change in dimensions of the lamellar micelle with increasing PLA block length.

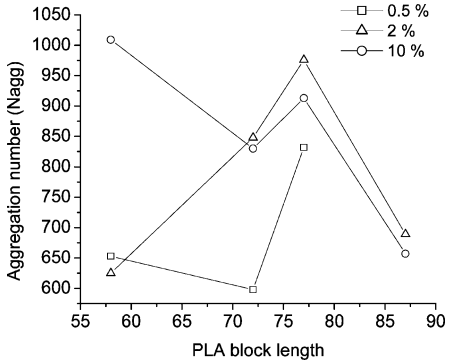

Figure 11. Change in aggregation number of the lamellar micelle with increasing PLA block length.

be in the range 12−16 nm and was seen to increase slightly with increasing PLA block length, except for the highest PLA length. Because of the large aggregation numbers leading to increased PEO density in the shell, the volume fraction of water in the shell is expected to be much lower in comparison to the *rac*-lactide series polymers. However the large sizes of the PEO layer cause the degree of hydration of the shell to be not significantly lower than the *rac*-lactide polymer micelles, except for the case of 58L polymers.

As stated previously, because of the random orientation of non-spherical "lamellar aggregates" and possible polydispersity in their sizes, a broad shoulder is observed for the L-lactide polymers instead of a correlation peak in the low q regime at high polymer concentrations. Hence, a characteristic correlation distance between "lamellar micelle" aggregates cannot be calculated directly from the scattering spectra. However the point where the shoulder begins to form in the low q region (q_{max}) gives us an estimate of the minimum size of the aggregates present in the system, which can be calculated as $D_{min} \sim 2\pi/q_{max}$. For all the L-lactide polymers at 30 wt % concentration, the value of D_{min} is approximately equal to or greater than 32 nm. This size obtained is in good agreement with the total aggregate sizes ($2L + d$) that we have obtained by data fitting for lower concentration samples. However, the model did not provide very good fits for the data at high concentrations of 22 and 30 wt %, and micellar structural parameters obtained from the fits were found to be inconsistent with the values obtained at lower concentrations. Hence, the data at high concentrations was fit by fixing the dimensions of the crystals (R and d) to that obtained from the low concentration data. The model did not describe the data very well at low q values for 22 and 30 wt % concentration samples where the structure factor effects are most prominent. It is possible that as the packing between micelles increases at high polymer concentrations, the individual

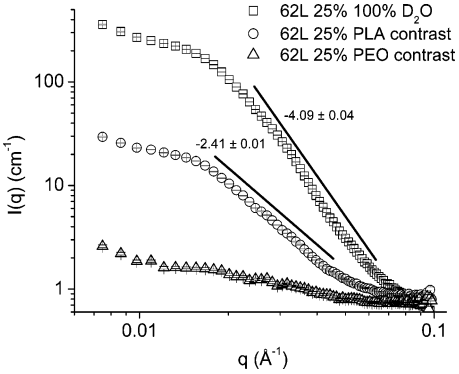

Figure 12. Scattering spectra obtained for 62L polymer at 25 wt % concentration and different solvent contrast conditions.

stacks of lamellar micelles are not distinguishable from each other and the scattering is obtained from randomly oriented micelles that are closely packed together. On the other hand, stacks of lamellae (values of $N > 1$) can be seen at low concentrations when they are distinguishable from each other.

Determination of Micellar Morphology by Contrast Matching Technique. In order to verify further the disk-like core−shell morphology of the "lamellar aggregates", we performed SANS under different contrast conditions to see either the core (PLA) or the shell (PEO) independently. As mentioned earlier the scattering length densities of PLA, PEO, D_2O, and H_2O are 1.79×10^{-6}, 6.39×10^{-7}, 6.36×10^{-6}, and -0.56×10^{-6}, respectively. Hence a mixture of 34% D_2O and 66% H_2O "matches" PLA, thereby making only the PEO visible to neutrons (PEO contrast), and at 17% D_2O and 83% H_2O, the PEO block is matched exactly making only the PLA visible (PLA contrast). We have shown the scattering spectra obtained for 62L polymer at 25 wt % under 100% D_2O contrast, PEO contrast, and PLA contrast conditions in Figure 12. The calculated slopes of the scattering spectra in the mid q region are indicated in the graph. The scattering spectra for the polymer aggregates under 100% D_2O contrast has a slope of -4.09 ± 0.04, which is close to the value of -4 expected for scattering from three-dimensional objects with sharp interfaces.[61] The small deviation from the value of -4 can be attributed to the diffuse boundary that the aggregates will have because of solvated PEO chains. Under the conditions when the SLD of the solvent is matched to that of PEO (PLA contrast), the scattering obtained is only due to the presence of PLA aggregates. The slope of the scattering spectra in this case is -2.41 ± 0.01. A slope of -2 is seen for two-dimensional objects with sharp interfaces and deviations from this value occur as the interface gets more diffuse or the bulk becomes more wrinkled. Since PLLA is semicrystalline, an increase in the slope of the scattering spectra from -2 to -2.41 may be caused because of the presence of amorphous PLA domains along with crystalline lamellae. A slope of -2.41 thus supports our observation that the L-lactide series polymers form two-dimensional disklike aggregates with solvated PEO chain attached on the face of PLA lamellae.

We fit the PLA contrast spectra to the model described by eqs 8, 9, and 10 using the SLD of the PLA and PEO as described above and the SLD of the solvent fixed to that of PEO. Under this condition, the layer thickness is not a variable and the model describes randomly oriented disklike structures formed by PLA scattered in the matrix formed by PEO and solvent with the only variables being the disk dimensions R and d and the total volume fraction of PLA. The model now has only four variables R, d, ϕ and background (bkg). The model fits the data well and

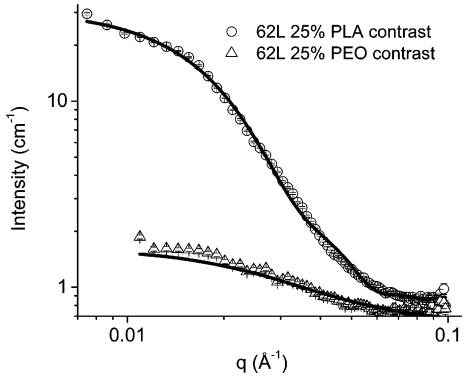

Figure 13. Fits of the (a) disklike core−shell model to 62L polymer at 25 wt % under PLA contrast condition and (b) Debye form factor for flexible Gaussian chains to 62L polymer at 25 wt % under PEO contrast condition

the fit is shown in Figure 13. The values obtained for R and d are 123 ± 1 and 86 ± 1 Å, respectively, which are in consonance with the values obtained for other L-lactide series polymers with similar MW at low polymer concentrations (Table 3).

The scattering spectra obtained under the condition of PEO contrast on the other hand is seen be similar to spectra obtained from flexible polymer chains in a good solvent (Figure 12). We thus fit this to the Debye expression for Gaussian chains[62] described as

$$I(q) = I(0)\frac{2[\exp(-x) - 1 + x]}{x^2} \qquad (14)$$

where x is equal to $q^2R_g^2$. The radius of gyration (R_g) of the PEO chains obtained from the fit of eq 14 to the data (Figure 13) is 57 ± 2 Å. The value of $2R_g$ is in excellent agreement with the total PEO layer thickness found by fitting the scattering data for 58L polymer in 100% D_2O contrast (Table 3). This agreement of the "lamellar micelle" structural parameters obtained independently for contrast matched SANS spectra and the SANS spectra in 100% D_2O establishes the effectiveness of the disklike core−shell model used in describing the scattering data.

Confidence in Analysis of L-lactide Series Data. Because of the lack of strong peaks in the L-lactide series data as well as deviations from the fits to the "lamellar micelles" model for high concentrations, it is valid to question our use of the "lamellar micelle" model as well as the actual fit parameters. We have strong confidence in our interpretation and analysis of the data for several reasons. We have mentioned these above, but summarize them again below.

(1) On the basis of our earlier studies using wide-angle X-ray diffraction (WAXD), we have shown that the L-lactide series polymers have crystalline domains in the hydrogel state due to crystalline PLLA.[30] A model for two-dimensional disklike shapes is a very reasonable and physical description of these nanocrystalline domains.

(2) Our results obtained by contrast matching experiments show that the micelle cores are indeed two-dimensional as evidenced by a slope of −2.4 in the mid and high q range, rather than in the range of −3 to −4 as we would expect for three-dimensional structures. In addition, data fits obtained for the sample with PEO contrast-matched independently yields parameters for dimensions of the core which are very similar to those obtained by fitting the data from samples in D_2O. It is also notable that, because of matching of the SLD of the solvent to that of PEO, the total number of parameters in the model were reduced to just three (R, d, and ϕ), thereby further establishing our confidence in the parameters obtained.

(3) There is a small degree of uncertainty in the values of micellar structural parameters R, d, and L obtained at lower concentrations (0.5%, 2%, and 10%), as demonstrated by the low relative error on these parameters (1−3%). The fits themselves are very sensitive to these as well as other model parameters. In addition, the values of the crystallite dimensions are in quantitative agreement with those obtained from XRD data.[59]

(4) Other models for different micellar geometries (e.g., spherical micelles) could not provide a satisfactory fit to the data. Some models do not even qualitatively fit the spectra for L-lactide polymers, yielding incorrect slopes in the mid and high q range. In other cases the parameters that we obtain from these models are unphysical. Thus, the disklike core−shell model provided not only a physically relevant description of the L-lactide polymer systems, but also was found to describe the data well, yielding parameters that could be analyzed to understand quantitatively the changes in nanoscale structure of the system with PLA block length.

Finally, we note that the quantitative values of structural parameters obtained for the L-series gels may vary slightly depending on the thermal history and/or processing conditions used to create the gels. We have derived crystallite sizes from XRD data on L-series gels quenched to different temperatures and have seen some variation in the dimensions.[59] However, all data are consistent with the basic picture of self-assembly into disklike micelles that we have described herein.

4. Conclusions

We have performed a detailed nanoscale structural characterization of PLA−PEO−PLA triblock copolymers in aqueous solution and gel state, and we have compared the structure of PLA−PEO−PLA polymers made from an amorphous racemic mixture of D- and L-lactide against that made from crystalline L-lactide. These studies complement our earlier structural studies of solutions and gels using WAXD,[30] ultra-small-angle X-ray scattering (USAXS), ultra-small-angle neutron scattering (USANS), and confocal microscopy;[63] and structural characterization of thin films using SAXS, diffraction, and optical microscopy.[64] The *rac*-lactide series polymers are seen to form flowerlike micelles in dilute solutions. With an increase in concentration of the polymer in solution, the hydrophobic end groups associate with the neighboring micelles to form a network of spherical micelles similar to what has traditionally been seen for ABA triblock copolymers in a solvent selective for the B-midblock. The crystalline L-lactide polymers form nonspherical micellar assemblies, which are similar in structure to lamellar micelles. The PLA end blocks associate between neighboring lamellae to form a network structure of randomly oriented lamellar micelles at higher concentrations, which leads to formation of very stiff hydrogels with high elastic modulus.[25] Data obtained from fits of physical models to the experimental data shows that the radius of spherical micelles formed for *rac*-lactide polymers lies in the range of 10−14 nm, whereas the size of PLA crystallites in L-lactide polymers is in the range of 11−15 nm in radius and 8−10 nm in thickness. The association properties of the polymer aggregates in solution are seen to be directly dependent upon the length and crystallinity of the hydrophobic PLA block. The changes in structure and association behavior of the gels upon changes in chemistry of the PLA block can be related to macroscopic and rheological properties

of the gels of these polymers in aqueous solution, thereby giving us a direct handle to design tailor-made materials useful for specific applications.

Acknowledgment. This material is based upon work partially supported by the National Science Foundation under Grant No. DMI-0531171. This work utilized facilities supported in part by the National Science Foundation under Agreement No. DMR-0454672. Support for this work was also provided by a 3M Nontenured Faculty Award and Dupont Young Professor Award to S.R.B. and an NIH Fellowship to N.S.-D. and a fellowship from the University of Massachusetts to S.K.A. as part of the Chemistry-Biology Interface Training Program (National Research Service Award T32 GM08515). We also acknowledge the support of J. Lal and E. Lang, Small Angle Scattering Instrument (SASI), Intense Pulse Neutron Source, Argonne National Lab, and L. Porcar at NCNR, NIST, for help with the neutron scattering experiments. We acknowledge the support of the National Institute of Standards and Technology, U.S. Department of Commerce, in providing the neutron research facilities used in portions of this work. Results shown in this report are partially derived from work performed at Argonne National Laboratory. Argonne is operated by UChicago Argonne, LLC, for the U.S. Department of Energy under Contract DE-AC02-06CH11357.

References and Notes

(1) Kubies, D.; Rypacek, F.; Kovarova, J.; Lednicky, F. *Biomaterials* **2000**, *21*, 529−536.
(2) Saito, N.; Okada, T.; Horiuchi, H.; Murakami, N.; Takahashi, J.; Nawata, M.; Ota, H.; Nozaki, K.; Takaoka, K. *Nat. Biotechnol.* **2001**, *19* (4), 332−335.
(3) Rashkov, I.; Manolova, N.; Li, S. M.; Espartero, J. L.; Vert, M. *Macromolecules* **1996**, *29*, 50−56.
(4) Molina, I.; Li, S. M.; Martinez, M. B.; Vert, M. *Biomaterials* **2001**, *22*, 363−369.
(5) Li, Y. X.; Volland, C.; Kissel, T. *J. Controlled Release* **1994**, *32*, 121−128.
(6) Li, Y. X.; Kissel, T. *J. Controlled Release* **1993**, *27*, 247−257.
(7) Lin, E. K.; Gast, A. P. *Macromolecules* **1996**, *29*, 4432−4441.
(8) Kissel, T.; Li, Y. X.; Unger, F. *Adv. Drug Delivery Rev.* **2002**, *54*, 99−134.
(9) Riley, T.; Heald, C. R.; Stolnik, S.; Garnett, M. C.; Illum, L.; Davis, S. S.; King, S. M.; Heenan, R. K.; Purkiss, S. C.; Barlow, R. J.; Gellert, P. R.; Washington, C. *Langmuir* **2003**, *19*, 8428−8435.
(10) Sun, L.; Ginorio, J. E.; Zhu, L.; Sics, I.; Rong, L. X.; Hsiao, B. S. *Macromolecules* **2006**, *39*, 8203−8206.
(11) Sun, L.; Zhu, L.; Rong, L. X.; Hsiao, B. S. *Angew. Chem., Int. Ed.* **2006**, *45*, 7373−7376.
(12) Park, M. J.; Char, K. *Langmuir* **2004**, *20*, 2456−2465.
(13) Semenov, A. N.; Joanny, J. F.; Khokhlov, A. R. *Macromolecules* **1995**, *28*, 1066−1075.
(14) Menchen, S.; Johnson, B.; Winnik, M. A.; Xu, B. *Chem. Mater.* **1996**, *8*, 2205.
(15) Xu, B.; Li, L.; Yekta, A.; Masoumi, Z.; Kanagalingam, S.; Winnik, M. A.; Zhang, K. W.; Macdonald, P. M. *Langmuir* **1997**, *13*, 2447−2456.
(16) Yekta, A.; Xu, B.; Duhamel, J.; Adiwidjaja, H.; Winnik, M. A. *Macromolecules* **1995**, *28*, 956−966.
(17) Tam, K. C.; Jenkins, R. D.; Winnik, M. A.; Bassett, D. R. *Macromolecules* **1998**, *31*, 4149−4159.
(18) Annable, T.; Buscall, R.; Ettelaie, R.; Whittlestone, D. *J. Rheol.* **1993**, *37*, 695−726.
(19) Kaczmarski, J. P.; Glass, J. E. *Macromolecules* **1993**, *26*, 5149−5156.
(20) Pham, Q. T.; Russel, W. B.; Thibeault, J. C.; Lau, W. *Macromolecules* **1999**, *32*, 5139−5146.
(21) Pham, Q. T.; Russel, W. B.; Lau, W. *J. Rheol.* **1998**, *42*, 159−176.
(22) Pham, Q. T.; Russel, W. B.; Thibeault, J. C.; Lau, W. *Macromolecules* **1999**, *32*, 2996−3005.
(23) Serero, Y.; Aznar, R.; Porte, G.; Berret, J. F.; Calvet, D.; Collet, A.; Viguier, M. *Phys. Rev. Lett.* **1998**, *81*, 5584−5587.
(24) Agrawal, S. K.; Sardhina, H. A.; Aamer, K. A.; Sanabria-DeLong, N.; Bhatia, S. R.; Tew, G. N. *ACS Symp. Ser.* **2006**, 924.
(25) Aamer, K. A.; Sardinha, H.; Bhatia, S. R.; Tew, G. N. *Biomaterials* **2004**, *25*, 1087−1093.
(26) Agrawal, S. K.; Chin, K. S.; Sanabria-DeLong, N.; Aamer, K. A.; Sardinha, H.; Tew, G. N.; Robert, S. C.; Bhatia, S. R. *Mater. Res. Soc. Symp. Proc.* **2005**, *844*, Y9.8.1−Y9.8.6.
(27) Winnik, M. A.; Yekta, A. *Curr. Opin. Colloid Interface Sci.* **1997**, *2*, 424−436.
(28) Agrawal, S. K.; Sanabria-DeLong, N.; Tew, G. N.; Bhatia, S. R. *J. Mater. Res.* **2006**, *21*, 2118−2125.
(29) Agrawal, S. K.; Sanabria-DeLong, N.; Tew, G. N.; Bhatia, S. R. *J. Controlled Release* **2006**, *112*, 64−71.
(30) Sanabria-DeLong, N.; Agrawal, S. K.; Bhatia, S. R.; Tew, G. N. *Macromolecules* **2006**, *39*, 1308−1310.
(31) Lee, D. S.; Shim, M. S.; Kim, S. W.; Lee, H.; Park, I.; Chang, T. Y. *Macromol. Rapid Commun.* **2001**, *22*, 587−592.
(32) Fujiwara, T.; Miyamoto, M.; Kimura, Y. *Macromolecules* **2000**, *33*, 2782−2785.
(33) Cao, L.; Manners, I.; Winnik, M. A. *Macromolecules* **2002**, *35*, 8258−8260.
(34) Fu, J.; Luan, B.; Yu, X.; Cong, Y.; Li, J.; Pan, C. Y.; Han, Y. C.; Yang, Y. M.; Li, B. Y. *Macromolecules* **2004**, *37*, 976−986.
(35) Xu, J. T.; Fairclough, J. P. A.; Mai, S. M.; Ryan, A. J. *J. Mater. Chem.* **2003**, *13*, 2740−2748.
(36) Richter, D.; Schneiders, D.; Monkenbusch, M.; Willner, L.; Fetters, L. J.; Huang, J. S.; Lin, M.; Mortensen, K.; Farago, B. *Macromolecules* **1997**, *30*, 1053−1068.
(37) Glinka, C. J.; Barker, J. G.; Hammouda, B.; Krueger, S.; Moyer, J. J.; Orts, W. J. *J. Appl. Crystallogr.* **1998**, *31*, 430−445. Thiyagarajan, P.; Epperson, J. E.; Crawford, R. K.; Carpenter, J. M.; Klippert, T. E.; Wozniak, D. G. *J. Appl. Crystallogr.* **1997**, *30*, 280−293.
(38) Huibers, P. D. T.; Bromberg, L. E.; Robinson, B. H.; Hatton, T. A. *Macromolecules* **1999**, *32*, 4889−4894.
(39) Goldmints, I.; von Gottberg, F. K.; Smith, K. A.; Hatton, T. A. *Langmuir* **1997**, *13*, 3659−3664.
(40) Yang, L.; Alexandridis, P.; Steytler, D. C.; Kositza, M. J.; Holzwarth, J. F. *Langmuir* **2000**, *16*, 8555−8561.
(41) Brown, G. J.; Richards, R. W.; Heenan, R. K. *Polymer* **2001**, *42*, 7663−7673.
(42) Chen, S. H. *Annu. Rev. Phys. Chem.* **1986**, *37*, 351−399.
(43) Glatter, O.; Scherf, G.; Schillen, K.; Brown, W. *Macromolecules* **1994**, *27*, 6046−6054.
(44) Mortensen, K.; Pedersen, J. S. *Macromolecules* **1993**, *26*, 805−812.
(45) Pedersen, J. S.; Svaneborg, C. *Curr. Opin. Colloid Interface Sci.* **2002**, *7*, 158−166.
(46) Svensson, B.; Olsson, U.; Alexandridis, P.; Mortensen, K. *Macromolecules* **1999**, *32*, 6725−6733.
(47) Pedersen, J. S.; Gerstenberg, M. C. *Macromolecules* **1996**, *29*, 1363−1365.
(48) Dozier, W. D.; Huang, J. S.; Fetters, L. J. *Macromolecules* **1991**, *24*, 2810−2814.
(49) Percus, J. K.; Yevick, G. J. *Phys. Rev.* **1958**, *110*, 1−13.
(50) BaggerJorgensen, H.; Coppola, L.; Thuresson, K.; Olsson, U.; Mortensen, K. *Langmuir* **1997**, *13*, 4204−4218.
(51) Tae, G. Y.; Kornfield, J. A.; Hubbell, J. A.; Lal, J. S. *Macromolecules* **2002**, *35*, 4448−4457.
(52) Liu, T. B.; Zhou, Z. K.; Wu, C. H.; Nace, V. M.; Chu, B. *Macromolecules* **1997**, *30*, 7624−7626.
(53) Milner, S. T.; Witten, T. A. *Macromolecules* **1992**, *25*, 5495−5503.
(54) Doi, M. *Introduction to polymer physics*; Clarendon Press; Oxford University Press: Oxford, U.K., and New York, 1996; pp ix, 120.
(55) Kanaya, T.; Ohkura, M.; Kaji, K.; Furusaka, M.; Misawa, M. *Macromolecules* **1994**, *27*, 5609−5615.
(56) Guinier, A.; Fornet, G. *Small-angle Scattering of X-rays*; Wiley: New York, 1955.
(57) Nelson, A.; Cosgrove, T. *Langmuir* **2004**, *20*, 2298−2304.
(58) Kratky, O.; Porod, G. *J. Colloid Science* **1949**, *4* (1), 35−70.
(59) Sanabria-Delong, N.; Agrawal, S. K.; Bhatia, S. R.; Tew, G. N. *Macromolecules* **2007**, *40*, 7864−7873.
(60) Vilgis, T.; Halperin, A. *Macromolecules* **1991**, *24*, 2090−2095.
(61) Higgins, J. S.; Benoît, H. *Polymers and neutron scattering*; Clarendon Press; Oxford University Press: Oxford, U.K., and New York, 1994; pp xix, 436.
(62) Debye, P. *J. Phys. Colloid Chem.* **1947**, *51* (1), 18−32.
(63) Agrawal, S. K.; Sanabria-DeLong, N.; Jemian, P. R.; Tew, G. N.; Bhatia, S. R. *Langmuir* **2007**, *23*, 5039−5044.
(64) Shin, D.; Shin, K.; Aamer, K. A.; Tew, G. N.; Russell, T. P.; Lee, J. H.; Jho, J. Y. *Macromolecules* **2005**, *38*, 104−109.

MA070634R